CASE REPORT

UDC: 616-006.2-07:616.831-006.2-073
DOI: 10.2298/VSP1203277M

Intracranial yolk sac tumor in an adult patient: MRI, diffusion-weighted imaging and ^{1}H MR spectroscopy features

Intrakranijalni *yolk sac* tumor kod odraslog bolesnika: karakteristike snimanja magnetnom rezonancom (MR), difuzionom MR i protonskom MR spektroskopijom

Marija Mačvanski*, Dragana Ristić-Baloš*, Brankica Vasić*, Slobodan Lavrnić*, Svetlana Gavrilović*, Mihajlo Milićević†, Sanja Milenković‡, Tatjana Stošić-Opinćal*

***Radiology and Magnetic Resonance Imaging Center, Clinical Center of Serbia, Belgrade, Serbia; †Neurosurgery Clinic, Clinical Center of Serbia, Belgrade, Serbia; ‡Pathology Department, Clinical Hospital Center Zemun, Belgrade, Serbia**

Abstract

Introduction. Yolk sac tumors represent only 5%–7% of intracranial germ cell tumors, which comprise about 1% of all primary brain tumors in adults. Literature data about nonspecific imaging characteristics of these tumors are scant. We presented magnetic resonance imaging findings with diffusion-weighted imaging and proton magnetic resonance spectroscopy of this rare type of tumor in an adult patient. **Case report.** A 55-year-old man with progressive left side weakness, headache, dizziness and ataxia, underwent preoperative magnetic resonance imaging, diffusion-weighted imaging and proton magnetic resonance spectroscopy. After surgical resection and histological analysis, the final diagnosis of yolk sac tumor was established. Retrospective imaging analysis were performed in order to determine imaging and biochemical parameters that could be useful in the diagnostic evaluation of this tumor type. **Conclusion.** Though the imaging features of yolk sac tumor are not specific, morphoanatomical and metabolic imaging could offer the information that provides new insights into this tumor that may facilitate further therapeutic decision process and potentially provides better information regarding the disease prognosis.

Key words:
brain neoplasms; endodermal sinus tumor; diagnosis; diagnostic techniques and procedures; magnetic resonance imaging; magnetic resonance spectroscopy; alpha-fetoproteins.

Apstrakt

Uvod. Tumori porekla žumančane kese (*yolk sac* tumori) predstavljaju samo 5–7% intrakranijalnih tumora porekla iz germinativnih ćelija, koji čine oko 1% svih primarnih tumora mozga kod odraslih. Podaci iz literature o nespecifičnim karakteristikama ovih tumora na snimku su oskudni. Prikazali smo nalaz magnetne rezonancije sa difuzionim snimanjem i protonskom magnetno-rezonantnom spektroskopijom ovog retkog oblika tumora kod odraslog bolesnika. **Prikaz bolesnika.** Bolesnik, star 55 godina, sa progresivnom levostranom slabošću, glavoboljom, vrtoglavicom i ataksijom, preoperativno je podvrgnut magnetnoj rezonanciji, difuzionom snimanju i protonskoj magnetno rezonantnoj spektroskopiji. Nakon hirurške intervencije i histološke analize, postavljena je konačna dijagnoza *yolk sac* tumora. Retrospektivna analiza snimanja sprovedena je sa ciljem određivanja parametara snimanja kao i biohemijskih parametara koji mogu biti korisni u dijagnostičkoj proceni ovog tipa tumora. **Zaključak.** Iako su karakteristike snimka *yolk sac* tumora nespecifične, morfoanatomsko i metaboličko snimanje može pružiti informacije koje daju novi uvid u ovu vrstu tumora, i time olakšati budući proces donošenja terapijske odluke. Osim toga, ono potencijalno obezbeđuje preciznije informacije, što je značajno za prognozu bolesti.

Ključne reči:
mozak, neoplazme; endodermalni sinus tumor; dijagnoza; dijagnostičke tehnike i procedure; magnetna rezonanca, snimanje; magnetna rezonanca, spektroskopija; alfa fetoproteini.

Correspondence to: Marija Mačvanski, Radiology and Magnetic Resonance Imaging Center, Clinical Center of Serbia, Pasterova 2, 11 000 Belgrade, Serbia. Phone: +381 11 361 5554. E-mail: macvanskimarija@yahoo.com

Introduction

Yolk sac tumors (YST) represent only 5%–7% of intracranial germ cell tumors (GCT), which comprise about 1% of all primary brain tumors in adults and 3%–8% of all primary brain tumors in children. The peak incidence of intracranial GCT is between 10 and 14 years, 95% of them occurring before the age of 35 [1–5]. Based on literature data, there are only two previously reported cases of patients with intracranial GCT elder than 45 years.

Since radiological appearance can be nonspecific and literature data of these tumors are scant, differentiation of YST from other neoplasms may be difficult. Conventional magnetic resonance imaging (MRI) with advanced MRI techniques, such as magnetic resonance diffusion [diffusion-weighted imaging (DWI) and proton magnetic resonance spectroscopy (^{1}H MRS)], can provide additional information to improve tumor characterization.

We reported the second case of YST and the third case of all intracranial GCT diagnosis in a 55-year-old patient using conventional MRI with DWI and ^{1}H MRS.

Case report

A 55-year-old man, was originally presented in March 2009, with a few-weeks history of progressive left side weakness, headache, dizziness and ataxia. Brain computed tomography (CT) scan showed expansive lesion with the localization on the right side of mesencephalon and cerebral peduncle. MRI revealed an expansive ovoid mass, 35 × 23 × 27 mm in size, localized in the region of the dorsal thalamus, cerebral peduncle, tegmentum mesencephali and ventral and proximal aspect of pons, dominantly on the right side. The tumor showed compression on the ventricle III and mediosagital structures with mild perifocal edema (Figure 1). The mass showed as heterogeneous, hypo- to isointense with hiperintense rim on T2-weighted (Figure 1a) and fluid-attenuated inversion-recovery (FLAIR), and hypointense with hiperintense focus on T1-weighted images (Figure 1b). The lesion displayed discretely enhancement (Figures 1c, d). DWI with calculated apparent diffusion coefficient (ADC) map revealed facilitated diffusion (1.44×10^{-3} mm^2 sec^{-1}) in the enhanced component of the lesion (Figure 2a). Multivoxel ^{1}H MRS with short echo time (TE = 30 ms) and selected voxel (Figures 2b, d) positioned in the rim of the lesion showed increased choline/creatine (Cho/Cr), decreased N-acetylaspartate/Cr (NAA/Cr) ratio and the presence of prominent lipid peak (Figures 2c, d). The radiological differential diagnosis included central nervous system (CNS) lymphoma and germinoma. Since the diagnosis of GCT was suspected, α-fetoprotein (AFP) and β-human chorionic gonadotropin (β-HCG) levels were checked preoperatively in the serum and cerebrospinal fluid (CSF). Laboratory tests showed normal values of AFP β-HCG in the serum (AFP: 7,46 ng/mL; β-HCG: 0,01 mIU/mL), and in the CSF (AFP: 0,56 ng/mL; β-HCG: 2,15 mIU/mL). Based on the extent of the lesion, no surgery was applied. Since biochemical analysis was negative, the patient underwent biopsy of the tumor in

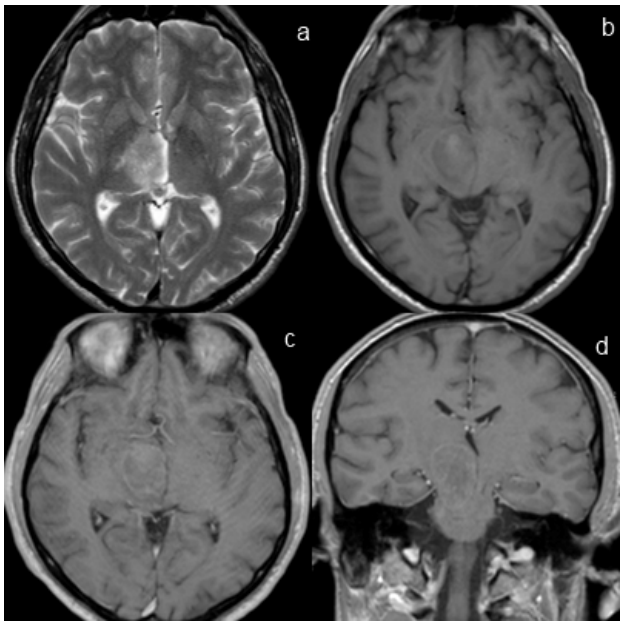

Fig. 1 – Tumor occupies dorsal thalamus, cerebral peduncle, mesencephalic tegmentum and pons with compromitation of third ventricle and adjacent structures Axial T2-weighted image (b) Axial T1-weighted image (c) Axial T1-weighted postcontrast image (d) Coronal T1-weighted postcontrast image

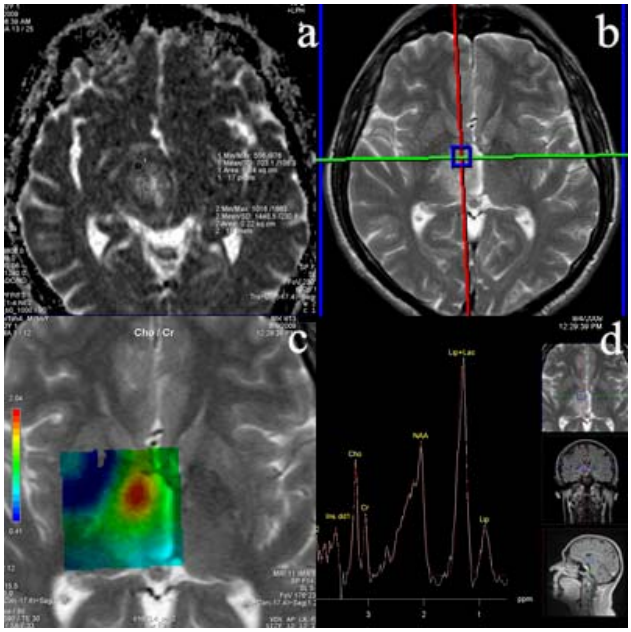

Fig. 2 – (a) Apparent diffusion coefficient (ADC) map with measured high ADC value; (b) One voxel from chemical shift imaging (CSI) position in the rim of the lesion, corresponding to an area of maximal choline/creatine (Cho/Cr) ratio; (c) Color map of CSI spectrum showing area of maximal Cho/Cr ratio with red color; (d) Spectrum from voxel corresponding to an area of maximal Cho/Cr ratio showing a marked decrease in N-acetylaspartate, increase in Cho and prominent lipids at 1.3 ppm

April 2009. Histological examination with immunohistochemistry showed polymorphic tumor proliferation, consisted of primitive epithelial cells, with isolated giant cells and hyaline globules within loose myxoid matrix (Figure 3a). The epithelial component of the tumor showed characteristic cytoplasmatic immunolabeling for AFP (Figure 3b). Since patient health status deteriorated, control brain CT and MRI were performed. Imaging findings showed progression of the lesion and the presence of hydrocephalus. A CSF shunt system was implanted, and antiedematose and hemiotherapy were introduced (CDDP Cisplatin, 35 mg). Five days after hemiotherapy, health state of the patient deteriorated for the second time and cardiac arrest emerged.

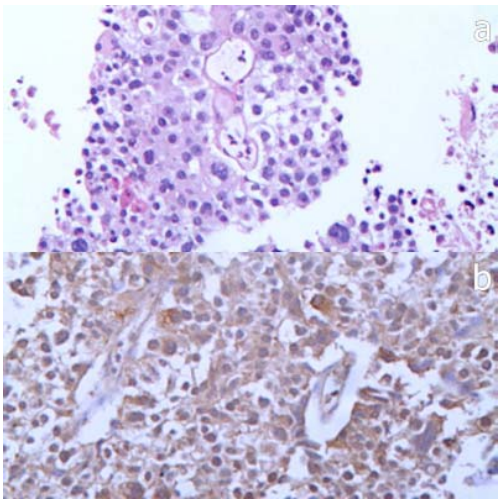

Fig. 3 – (a) Polymorphism, primitive appearing epithelial cells and hyaline globules in yolk sac tumor (YST) (H&E × 20); (b) the alpha fetoprotein (AFP) cytoplasmatic immunolabeling of YST epithelial component (AFP × 20)

Discussion

The World Health Organization classificated intracranial GCT as: germinomas, embryonal carcinomas, YST (s. endodermal sinus tumors), choriocarcinomas, teratomas (mature and immature), teratomas with malignant transformation and mixed germ cell tumors [2]. Intracranial GCT comprises about 1% of all primary brain tumors in adults [2–7] and 3%–8% of all primary brain tumors in children [8–12]. Among all primary intracranial GCT, the most common histological types are germinomas (60%), while YST represent only 5%–7% of these tumors [2, 5]. The peak incidence of intracranial GCT is between 10 and 14 years, and almost 95% of these tumors occur before the age of 35 [1–5]. Although the vast majority of cases are diagnosed in young children, there have been isolated case reports in adults. Kirikae et al. [13] reported the eldest patient with intracranial GCT who was a 65-year-old man with YST. Park and al. [14] reported a 47-year-old woman with intracranial mature teratoma. Based on literature data, our case is the second one with YST and the third one of all intracranial GCT in a patient elder than 45 years.

The biochemical assessment of intracranial GCT serves as an accepted method for initial classification without tissue sampling, while CSF cytology is an evidence of tumor dissemination into the neuroaxis [14–17]. Laboratory diagnosis of GCT is based on tumor markers analysis in the serum and CSF, and CSF cytology [2, 3]. The normal range of AFP in the serum and CSF for adults is 0–15 ng/mL, and normal serum and CSF β-HCG levels are less than 2,5 mIU/mL in men, and less than 5,0 mIU/mL in non-pregnant women [14–17]. Associated predominantly with YST, AFP can also be expressed by embryonic carcinomas and immature teratomas, while β-HCG is markedly elevated in association with choriocarcinomas and germinomas with the presence of syncytiotrophoblastic giant cells [14–17]. Although YST is known to be an AFP-producing tumor, our patient showed normal values of AFP. As in other cases, production of β-HCG was not present in our case, too.

As typical for GCT, YST arises as midline tumors, commonly localized in the pineal or suprasellar region [5–11]. Since radiological manifestation can be nonspecific, especially in adults, differentiation of YST from other neoplasms is difficult [18, 19]. Literature data of YST, especially about their radiological appearance, are scant [1, 2, 17, 18, 20–22]. On MRI, YST is usually shown as heterogeneous mass with foci of calcification and cysts, and contrast enhancement [1, 2]. As in our case, there are cases described with T1-weighted iso-/hypointense and T2-weighted iso/hyperintense appearance of these tumors [20–23]. MRI presentation of our case only confirms unspecific manifestation of YST. Based on conventional MRI findings, differential diagnosis included primary CNS lymphoma and germinoma. Advanced MR techniques offered additional information which could improve tumor characterization. Based on ^{1}H MRS lymphoma and germinoma were highly suspected. Like in lymphomas and germinomas [21], ^{1}H MRS of YST showed increased Cho/Cr, decreased NAA/Cr ratio and the presence of prominent lipid peak. Since ^{1}H MRS of these tumors is very similar, usefulness of these findings was limited. Lipid resonances may originate from mobile lipid molecules, based on tissue degradation and necrosis, or from B-lymphocytes, transformed T-lymphocytes, cultured human leukemic lymphocytes and macrophages [24]. A strongly increased Cho/NAA ratio and lipid resonances in the absence of necrotic area on MRI, is suggestive for lymphocytes infiltration. However, based on DWI, differential diagnosis can be made. DWI evaluates size of extracellular space, cellularity and cytoplasm/extracellular space ratio [25]. Intracranial primary lymphomas show restrictive diffusion due to their hipercelullarity [2, 5, 21]. Similar to lymphomas, germinomas demonstrate restrictive diffusion with low ADC values [2, 5]. Unlike lymphomas and germinomas, YST shows facilitated diffusion. This information is important for MR diagnosis of YST, and consequently for patient's therapeutic treatment and prognosis.

While germinomas are exquisitely radiosensitive, with a 5-year survival rates of roughly 90% with radiotherapy alone, for other intracranial GCT neoadjuvant chemotherapy is used in combination with radiotherapy and maximal surgical resection. YST, like most of other GCT, are associated

with the poorest prognosis, with a 5-year survival rates in the range of 9% to 49%, even with aggressive therapy [2, 7, 15, 26, 27].

Conclusion

There are no specific imaging features of YST, but DWI and ^{1}H MRS offer information that provides new insights into these tumors, and may play the role in differentiation from other neoplasms. Still, histological verification remains necessary.

Conflict of interest statement

The authors declare that there is no conflict of interest.

R E F E R E N C E S

1. *Hedlund GL*. Germ Cell Tumors. In: *Osborn AG*, *Blaser* SI, *Salzman KL*, *Katzman GL*,. *Provenzale J*, *Castillo M*, et al, editors. Diagnostic imaging: brain. 1st ed. Salt Lake City, Utah: Amirsys; 2004. p. 463−6.
2. *Illner A*. Pineal Parenchymal Tumors. In: *Osborn AG*, *Blaser* SI, *Salzman KL*, *Katzman GL*,. *Provenzale J*, *Castillo M*, et al, editors. Diagnostic imaging: brain. 1st ed. Salt Lake City, Utah: Amirsys; 2004; p. 511−8.
3. *Rosenblum MK, Nakazato Y, Matsutani M*. CNS germ cell tumours. In: Louis DN, Ohgaki H, Wiestler OD, Cavenee WK, editors. WHO Classification of Tumours of the Central Nervous System. Lyon, France: IARC; 2007, p. 198−204.
4. *Echevarría ME, Fangusaro J, Goldman S*. Pediatric central nervous system germ cell tumors: a review. Oncologist 2008; 13(6): 690−9.
5. *Villano JL, Virk IY, Ramirez V, Propp JM, Engelhard HH, McCarthy BJ*. Descriptive epidemiology of central nervous system germ cell tumors: nonpineal analysis. Neuro Oncol 2010; 12(3): 257−64.
6. *Jennings MT, Gelman R, Hochberg F*. Intracranial germ-cell tumors: natural history and pathogenesis. J Neurosurg 1985; 63(2): 155−67.
7. *Matsutani M*. Pineal germ cell tumors. Prog Neurol Surg 2009; 23: 76−85.
8. *Kyritsis AP*. Management of primary intracranial germ cell tumors. J Neurooncol 2010; 96(2): 143−9.
9. *Göbel U, Schneider DT, Calaminus G, Haas RJ, Schmidt P, Harms D*. Germ-cell tumors in childhood and adolescence. GPOH MAKEI and the MAHO study groups. Ann Oncol 2000; 11(3): 263−71.
10. *Glezer A, Paraiba DB, Bronstein MD*. Rare sellar lesions. Endocrinol Metab Clin North Am 2008; 37(1): 195−211, x.
11. *Ozelame RV, Shroff M, Wood B, Bouffet E, Bartels U, Drake JM,* et al. Basal ganglia germinoma in children with associated ipsilateral cerebral and brain stem hemiatrophy. Pediatr Radiol 2006; 36(4): 325−30.
12. *Tsugu H, Oshiro S, Ueno Y, Abe H, Komatsu F, Sakamoto S*, et al. Primary yolk sac tumor within the lateral ventricle. Neurol Med Chir (Tokyo) 2009; 49(11): 528−31.
13. *Kirikae M, Arai H, Hidaka T, Kidoguchi J, Miura K, Kitakami A,* et al. Pineal yolk sac tumor in a 65-year-old man. Surg Neurol 1994; 42(3): 253−8.
14. *Park KB, Park HS, Lee JI, Suh YL*. Mature teratoma in the cerebellar hemisphere of an adult. J Korean Neurosurg Soc 2007; 41(3): 180−1. (Korean)
15. *Luther N, Edgar MA, Dunkel IJ, Souweidane MM*. Correlation of endoscopic biopsy with tumor marker status in primary intracranial germ cell tumors. J Neurooncol 2006; 79(1): 45–50.
16. *Blakeley JO, Grossman SA*. Management of pineal region tumors. Curr Treat Options Oncol 2006; 7(6): 505−16.
17. *Cheng CM, Chiang YH, Nieh S*. Pineal region teratoma with high serum and CSF alpha-fetoprotein levels. J Clin Neurosci 2006; 13(2): 257−9.
18. *Davaus T, Gasparetto EL, Carvalho Neto A, Jung JE, Bleggi-Torres LF*. Pineal yolk sac tumor: correlation between neuroimaging and pathological findings. Arq Neuropsiquiatr 2007; 65(2A): 283−5.
19. *Hirato J, Nakazato Y*. Pathology of pineal region tumors. J Neurooncol 2001; 54(3): 239−49.
20. *Balmaceda C, Finlay J*. Current advances in the diagnosis and management of intracranial germ cell tumors. Curr Neurol Neurosci Rep 2004; 4(3): 253−62.
21. *Smirniotopoulos JG, Rushing EJ, Mena H*. Pineal region masses: differential diagnosis. Radiographics 1992; 12(3): 577−96.
22. *Verma R, Malone S, Canil C, Jansen G, Lesiuk H*. Primary skull-based yolk-sac tumour: case report and review of central nervous system germ cell tumours. J Neurooncol 2011; 101(1): 129−34.
23. *Al-Okaili RN, Krejza J, Wang S, Woo JH, Melhem ER*. Advanced MR imaging techniques in the diagnosis of intraaxial brain tumors in adults. Radiographics 2006; 26 Suppl 1: S173−89.
24. *Korogi Y, Takahashi M, Ushio Y*. MRI of pineal region tumors. J Neurooncol 2001; 54(3): 251−61.
25. *Luther N, Greenfield JP, Chadburn A, Schwartz TH*. Intracranial nasal natural killer/T-cell lymphoma: immunopathologically-confirmed case and review of literature. J Neurooncol 2005; 75(2): 185−8.
26. *Douglas-Akinwande AC, Ying J, Momin Z, Mourad A, Hattab EM*. Diffusion-weighted imaging characteristics of primary central nervous system germinoma with histopathologic correlation: a retrospective study. Acad Radiol 2009; 16(11): 1356−65.
27. *Ogawa K, Toita T, Nakamura K, Uno T, Onishi H, Itami J*, et al. Treatment and prognosis of patients with intracranial nongerminomatous malignant germ cell tumors: a multiinstitutional retrospective analysis of 41 patients. Cancer 2003; 98(2): 369−76.

Received on July 30, 2010.
Accepted on November 15, 2010.